RSC Advances

This is an *Accepted Manuscript*, which has been through the Royal Society of Chemistry peer review process and has been accepted for publication.

Accepted Manuscripts are published online shortly after acceptance, before technical editing, formatting and proof reading. Using this free service, authors can make their results available to the community, in citable form, before we publish the edited article. This *Accepted Manuscript* will be replaced by the edited, formatted and paginated article as soon as this is available.

You can find more information about *Accepted Manuscripts* in the Information for Authors.

Please note that technical editing may introduce minor changes to the text and/or graphics, which may alter content. The journal's standard Terms & Conditions and the Ethical guidelines still apply. In no event shall the Royal Society of Chemistry be held responsible for any errors or omissions in this *Accepted Manuscript* or any consequences arising from the use of any information it contains.

ROYAL SOCIETY OF CHEMISTRY

www.rsc.org/advances

Structure and electrical properties of $Bi_{1/2}Na_{1/2}TiO_3$-based lead-free piezoelectric ceramics

Renfei Cheng[1], Zhijun Xu[1*], Ruiqing Chu[1], Jigong Hao[1], Juan Du[1], Guorong Li[2]

1. College of Materials Science and Engineering, Liaocheng University, Liaocheng 252059, People's Republic of China

2. The State Key Lab of High Performance Ceramics and Superfinemicrostructure, Shanghai Institute of Ceramics, Chinese Academy of Science, Shanghai 200050, People's Republic of China

Abstract: Lead-free piezoelectric ceramics $(1-x)(0.935Bi_{1/2}Na_{1/2}TiO_3-0.065BaTiO_3)-xAl_6Bi_2O_{12}$ (BNT-BT6.5-x AB, with x=0-0.020) were prepared using a conventional solid-state reaction method and the crystal structure and electrical properties were systematically investigated. All BNT-BT6.5-x AB ceramics form the pure perovskite phase structure, SEM-analysis revealed an increase first and then decrease in the grain size with increasing AB content with no obvious change in grain morphology. Appropriate AB doping into BNT-BT6.5 ceramics induce the enhancement of piezoelectric and ferroelectric properties. Improved P_r = 32.8 μC/cm^2, low E_c of 18.2 kV/cm, and high d_{33} = 234 pC/N were observed at x = 0.005. Furthermore, electric field-induced strain was enhanced to its maximum value (S_{max} = 0.33%) with normalized strain ($d^*_{33} = S_{max}/E_{max}$ = 413 pm/V) at an applied electric field of 80 kV/cm for x = 0.010. The enhanced strain can be attributed to the coexistence of ferroelectric and relaxor ferroelectric phases. It is obvious that this piezoceramic is promising candidate for lead-free piezoceramic and can be used in practical applications.

Keywords: Piezoceramics; Structure; Electrical properties

1. Introduction

Traditional lead-based piezoelectric ceramics with perovskite structures, such as $Pb(Co_{1/3}Nb_{2/3})O_3$-$PbTiO_3$-$PbZrO_3$[1] and $Pb(Mg_{1/3}Nb_{2/3})O_3$-$PbTiO_3$-$PbZrO_3$,[2] have been widely applied in modern piezoelectric devices owing to their excellent electrical properties.[3, 4] However, the high

* Corresponding author. Tel. / fax: +86 635 8230923. E-mail address: zhjxu@lcu.edu.cn.

RSC Advances Accepted Manuscript

volatility and strong toxicity of lead oxide during sintering have caused severe ecological and environmental problems.[5, 6] Therefore, extensive efforts have been done to find a promising way to solve this problem and develop new lead-free piezoelectric ceramics with excellent properties to replace lead based ceramics.[7, 8] Recently, experimental studies on $(Bi_{1/2}Na_{1/2})TiO_3$ (BNT) have been performed extensively. BNT is considered to be an excellent candidate of lead-free piezoelectric ceramics because of its strong ferroelectric properties (P_r = 38 μC/cm^2) at room temperature and high Curie temperature of 320°C. However, the use of pure BNT materials in piezoelectric application is limited by the difficulty to pole adequately due to its large coercive fields (E_c = 73kV/cm) and comparatively large conductivity. [9-11] A multitude of efforts have been made in order to improve the performance of BNT by forming BNT-based solid solutions.

To improve piezoelectric and ferroelectric properties of BNT ceramics, a variety of researches for a new morphotropic phase boundary (MPB) in the BNT-based solid solutions, e.g. BNT-$BaTiO_3$, [12,13] and BNT-$Bi_{1/2}K_{1/2}TiO_3$, [14,15] have been concentrated in recent years. It is well known that the MPB plays a very important role in PZT ceramics because the piezoelectric and ferroelectric properties show a maximum over a specific compositional range around the MPB. Among these solid solutions, $(1-x)(Bi_{1/2}Na_{1/2})TiO_3$-$x$$BaTiO_3$(BNT-$x$BT) system, similar to the $(1-x)PbZrO_3$-$x$$PbTiO_3$ ceramics, [16] has been attracted considerable attention owing to the existence of a rhombohedral–tetragonal MPB near x=0.06-0.07 [17] and its enhanced ferroelectric and electromechanical properties at this boundary. [18] The composition x=0.065 for BNT-xBT ceramics belongs to the region of MPB, which has a relative high piezoelectric and ferroelectric properties. [19] However, the piezoelectric properties of BNT-BT system are not good enough for practical uses. In order to further enhance the properties of BNT-BT ceramics and meet the requirements for practical uses, it is necessary to develop new BNT-based ceramics.

RSC Advances Accepted Manuscript

Theoretical studies predict that $BiAlO_3$ has been predicted to be promising candidate for lead-free ferroelectric materials because of their large ferroelectric polarization and piezoelectricity by theoretical calculations.[20] However, $BiAlO_3$ has to be prepared at high pressure and high temperature conditions.[21] Consequently, a host of studies have been made in which $BiAlO_3$ has been used as an addition to enhance the performance of BNT-based in the form of solid solution.[22] The results implied that BNT-based ceramics with $BiAlO_3$-doping could be excellent lead-free candidates for ferroelectric material. Yu et al. have synthesized and studied BNT-$BiAlO_3$ solid solution.[23] Zhen et al.[24] reported that $Al_6Bi_2O_{12}$ doped BNT enhanced ferroelectric and piezoelectric properties and increased the Cure temperature, simultaneously decreased the coercive field. Fu et al.[25] have observed that the addition of $BiAlO_3$ to BNT-BT can moderate relative dielectric constant. Based on the above results, it is expected that the $Al_6Bi_2O_{12}$ doped $0.935Bi_{1/2}Na_{1/2}TiO_3$-$0.065BaTiO_3$ (BNT-BT6.5) can improve the ferroelectric and piezoelectric properties with higher Curie temperature and higher field-induced strain.

In this work, we doped BNTBT-6.5 with $Al_6Bi_2O_{12}$ (AB) using a conventional solid-state reaction method and we systematically studied the influence of compositional modification on the crystal structure, ferroelectric and piezoelectric properties and field-induced strain behaviors.

2. Experimental procedure

The produced materials $(1-x)(0.935Bi_{1/2}Na_{1/2}TiO_3-0.065BaTiO_3)-xAl_6Bi_2O_{12}$ (BNT-BT6.5-*x*AB, with x=0-0.020) were prepared by the conventional solid-state reaction method using reagent-grade metal oxides or carbonate powders of Bi_2O_3 (99%), TiO_2 (99.5%), Na_2CO_3 (99.8%), $BaCO_3$ (99%) and Al_2O_3(99.5%) as starting materials. All raw materials made by Sinopharm Chemical Reagent Co. Ltd. were weighed at stoichiometric proportion and then mixed homogenized by planetary ball milling in a polyethylene with stabilized zirconia balls for 12 h, using anhydrous ethanol as liquid medium. After

RSC Advances Accepted Manuscript

drying, the mixed powders were calcined at 850°C for 2 h. After calcination, the mixture was milled again for 6 h. The powders were mixed with an appropriate amount of polyvinyl butyral (PVB) binder, and pressed into pallets with a diameter of 12 mm and a thickness of 1.0 mm under the pressure of about 200 MPa. After burning off PVB, the ceramics were sintered in an alumina crucible at 1100–1180 °C for 2 h in air. To reduce the loss of bismuth and sodium oxides during sintering, the pellets were embedded into preprepared powder with the same composition.

The crystal structure of the ceramics was determined by X-ray diffraction (XRD) using a Cu K_α radiation (λ=1.54178 Å) (D8 Advance, Bruker Inc., Germany). The surface morphology of the ceramics was observed by scanning electron microscope (SEM) (JSM-6380, Japan). Silver electrodes were coated on the top and bottom surfaces of the ceramics for the subsequent electrical measurements. *P-E* loops and *S-E* curves, where *P*, *E*, and *S* denote the polarization, the electric field and the strain, respectively, were measured with ferroelectric analyzer (TF2000 analyzer, Aixacct, Germany) along with the laser interferometer (SIOS Meßtechnik GmbH, Germany) under an electric field of 80 kV/cm. The temperature dependence of dielectric properties was measured using a Broadband Dielectric Spectrometer (Novocontrol Germany) at temperatures ranging from room temperature to 500°C with a heating rate of 3 °C/min. The samples were poled in silicon oil at room temperature under 50–70 kV/cm for 20 min, and piezoelectric measurements were then carried out using a quasi-static d_{33}-meterYE2730 (SINOCERA, China).

3. Results and discussion

RSC Advances Accepted Manuscript

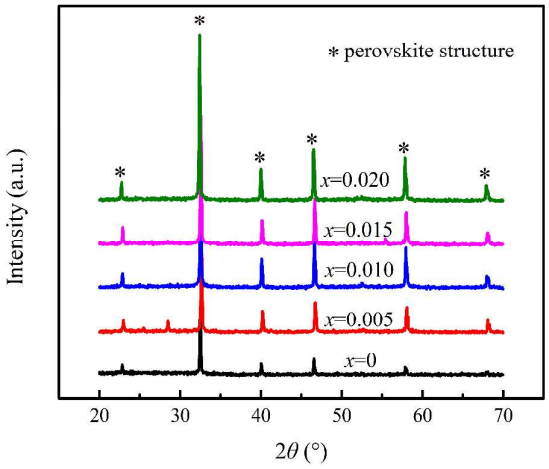

Fig. 1 X-ray diffraction patterns of BNT-BT6.5-*x* AB with *x*=0-0.020.

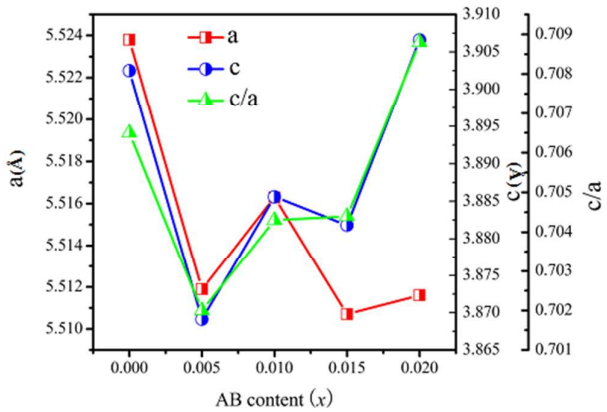

Fig.2 Lattice parameters a, c and c/a as a function of AB contents *x* for the BNT-BT6.5-*x*AB ceramics

Fig. 1 shows X-ray diffraction patterns of BNT-BT6.5-*x* AB ceramics sintered at 1150 °C. It can be seen that all samples have formed the pure perovskite phase without any traces of secondary phases, as shown in **Fig. 1**, implying that AB has diffused into the BNT-BT6.5 ceramics lattice or the second phase cannot be detected because of the small doping amount of AB. These results indicate that the addition of AB does not lead to an obvious change in the phase structure. **Fig. 2** shows the lattice constants a, c, and c/a as functions of the amount of AB in BNT-BT6.5 ceramics. Lattice constant *a* decreased with increasing AB amount, while lattice constant *c* was found to increase first and then

RSC Advances Accepted Manuscript

decrease. The general trend of c/a ratio gradually increased with increasing AB content, suggesting the enhancement of tetragonality.

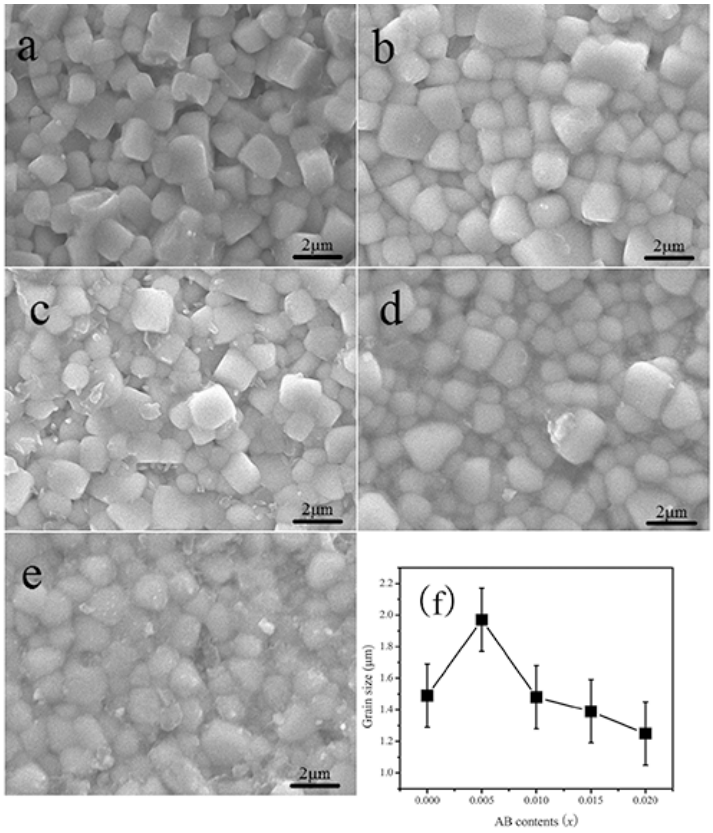

Fig. 3 SEM micrographs of the BNT-BT6.5-*x*AB ceramics sintered at 1150°C for 2 h: a $x = 0$, b $x = 0.005$, c $x = 0.010$, d $x = 0.015$ and e $x = 0.020$; (f) the dependence of Grain size on x

The microstructures of all the sintered samples ($0 \leqq x \leqq 0.02$) are depicted in **Fig. 3.** It can be noticed that all ceramics are dense and have uniform and compact structure. AB addition into BNT-BT6.5-*x*AB is found to slightly increase the grain size and then decrease it. The average grain size of these samples has been determined by line intercept method (see **Fig. 3(f)**). At the same time, the elemental concentrations of all samples were analyzed by EDS. Although EDS is not a very precise method for quantitative analysis at low concentration, the contents of AB increase and the peaks of Al in EDS spectrum show more and more obviously with the increase of x. **Fig. 4** shows the representative results of the EDS analysis for the BNT-BT6.5-*x*AB piezoceramics with $x = 0.005$ and $x = 0.010$. The

RSC Advances Accepted Manuscript

region enclosed by the line in the inset of the figure was analyzed, which confirmed the existence of Al element in the sintered samples.

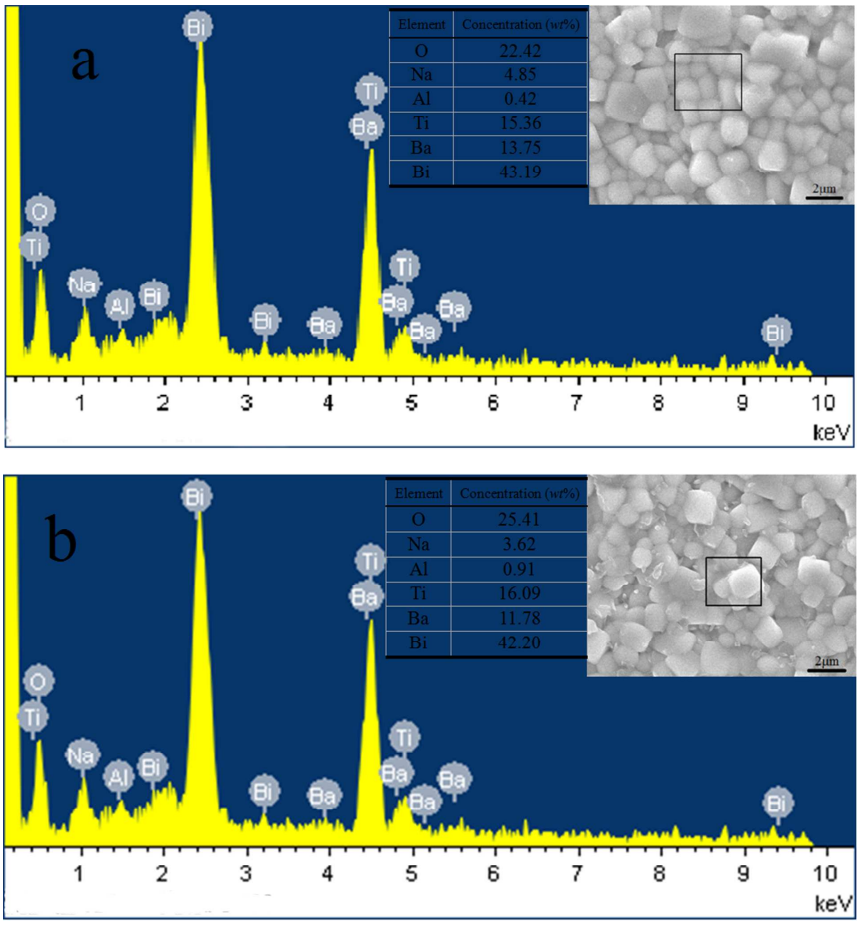

Fig. 4 Elemental concentrations of BNT-BT6.5-*x*AB ceramics by EDS analysis: a $x = 0.005$, b $x = 0.010$

RSC Advances Accepted Manuscript

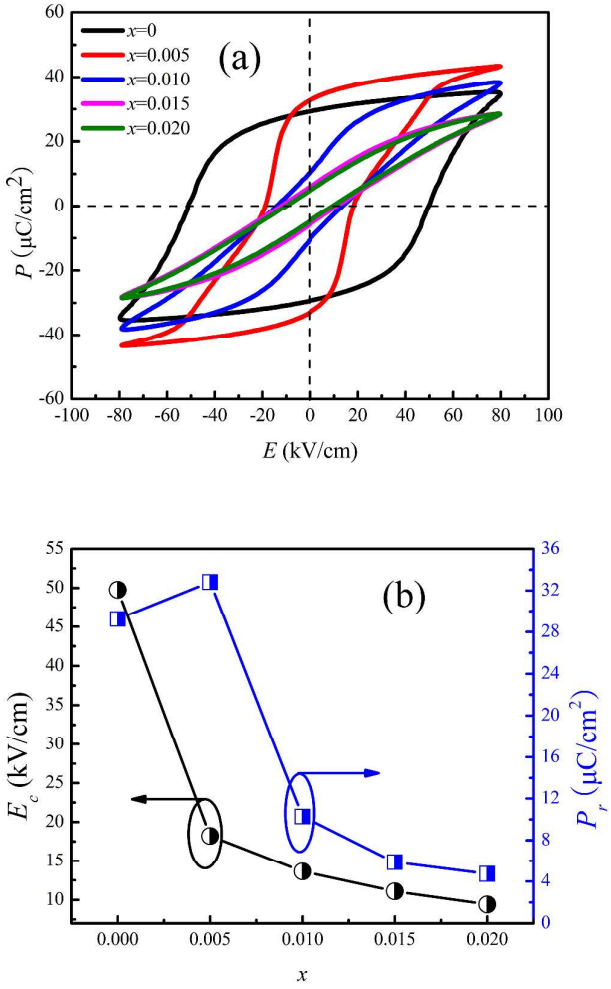

Fig.5 (a) Room-temperature *P* - *E* hysteresis loops of all BNT-BT6.5-*x* AB ceramics, **(b)** variation in remnant polarization (P_r) and coercive field (E_c) as a function of *x*

Hysteresis loops (*P*-*E*) of BNT-BT6.5-*x*AB ceramics with $0 \leq x \leq 0.020$ measured at room temperature at 10 Hz are shown in **Fig.5 (a)**. The *P*-*E* shape strongly depends on the composition of the ceramics. Detailed information on the response of the variation of P_r and E_c of BNT-BT6.5-*x*AB ceramics as a function of *x* is provided in **Fig.5 (b)**. The BNT-BT6.5 ceramic exhibits typical ferroelectric behavior with P_r and E_c values of 29.3μC/cm^2 and 49.7 kV/cm, respectively. As *x* increases, the P_r increases and then decreases while E_c drops dramatically. At x =0.005, the value of P_r reaches a maximum value of 32.8μC /cm^2 with E_c of 18.2 kV/cm. With *x* further increasing to 0.010, the *P*-*E* loop becomes exceedingly flattened and slanted, implying that excess AB addition greatly

RSC Advances Accepted Manuscript

weakens the ferroelectricity of the samples.

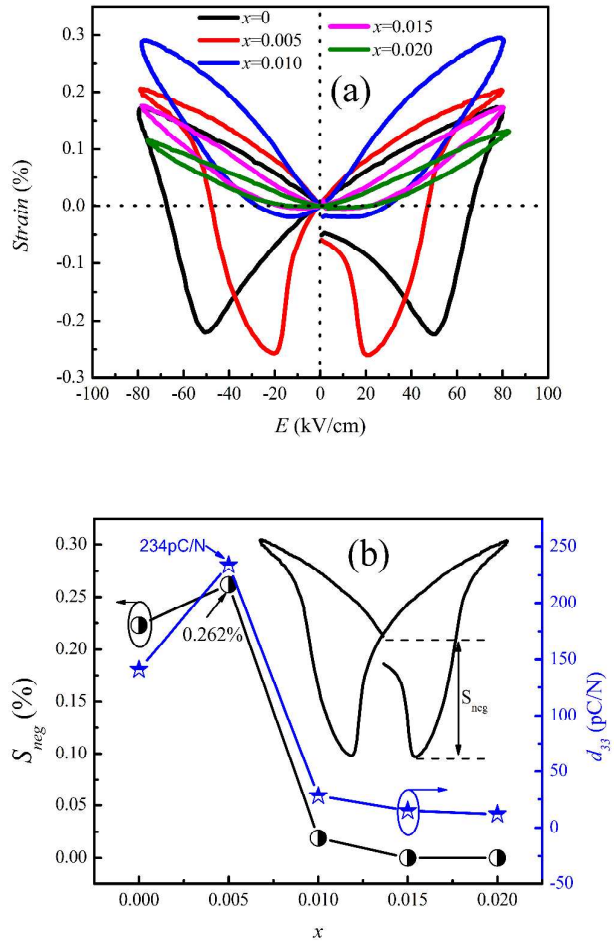

Fig. 6 (a) Field induced bipolar *S*-*E* loops of BNT-BT6.5 ceramics with different AB contents, **(b)** negative strain (S_{neg}) and piezoelectric constant (d_{33}) of BNT-BT6.5 ceramics as a function of AB content

Fig. 6 (a) shows the bipolar field-induced strain curves of BNT-BT6.5-*x*AB ceramics measured at room temperature under an applied electric field of 80 kV/cm. Pure BNT-BT6.5 ceramic exhibits a typical butterfly-shaped curve with a maximum strain (S_{max}) of 0.17% and negative strain (S_{neg}) of 0.22% indicating a ferroelectric order. With x increasing (i.e., x = 0.010), the curves change shape, resulting in an increase in the maximum strain and a concurrent decrease in the negative strain. At x=0.010, a significant enhancement in strain (S_{max} = 0.29 %) was observed. However, above this critical

RSC Advances Accepted Manuscript

composition (x = 0.010), drastic changes from the typical ferroelectric order were observed. This was evidenced by the absence of a negative strain, which is the difference between the zero-field strain and the lowest strain and is closely related to domain back-switching during bipolar cycles.[26] The trend for the negative strain level (S_{neg}) and the piezoelectric constant (d_{33} = pC/N) of BNT-BT6.5-x AB ceramics are presented in **Fig. 6(b)**. The d_{33} first increased up to x=0.005 ceramics with a maximum value of 234 pC/N, which is larger than those of BNT-BT ceramics with other additives [27, 28]. Further increase in AB concentration resulted in a significant reduction in d_{33}. Generally, the piezoelectric properties of samples are determined by the microstructure and phase structure.[29] For small amount of AB, increase of grain size is beneficial for the enhancement of d_{33}.[29] However, the excess AB may precipitate in the grain boundary, which may lead to the accumulation of space charges, thus limiting the movement of the domains.[29, 30] For BNT-BT6.5-0.005AB ceramics, similar to BNT-x BT binary ceramics, it may have a rhombohedra-tetragonal MPB in the range of 0.06-0.07 and reveal relatively high piezoelectric and ferroelectric properties at the composition near the MPB. The large enhancement in piezoelectric properties of the BNT-BT6.5-0.005AB ceramics can be attributed to the existence of the MPB because the number of possible spontaneous polarization directions increase at the MPB.[31] Similar trends in S_{neg} were observed which increased up to 0.26% for x=0.005 ceramic and then decreases. The observed trends of d_{33} and S_{neg} are in good agreement with P-E hysteresis loops as shown in **Fig. 5(a)**; similar behavior is also observed in other studies.[25, 32] The substantial increase in d_{33} at x=0.005 is attributed to a large remnant polarization (P_r) and a lower coercive field (E_c). This is because a lower E_c enables the ceramics to be more easily poled, whereas a large P_r favors piezoelectricity.

RSC Advances Accepted Manuscript

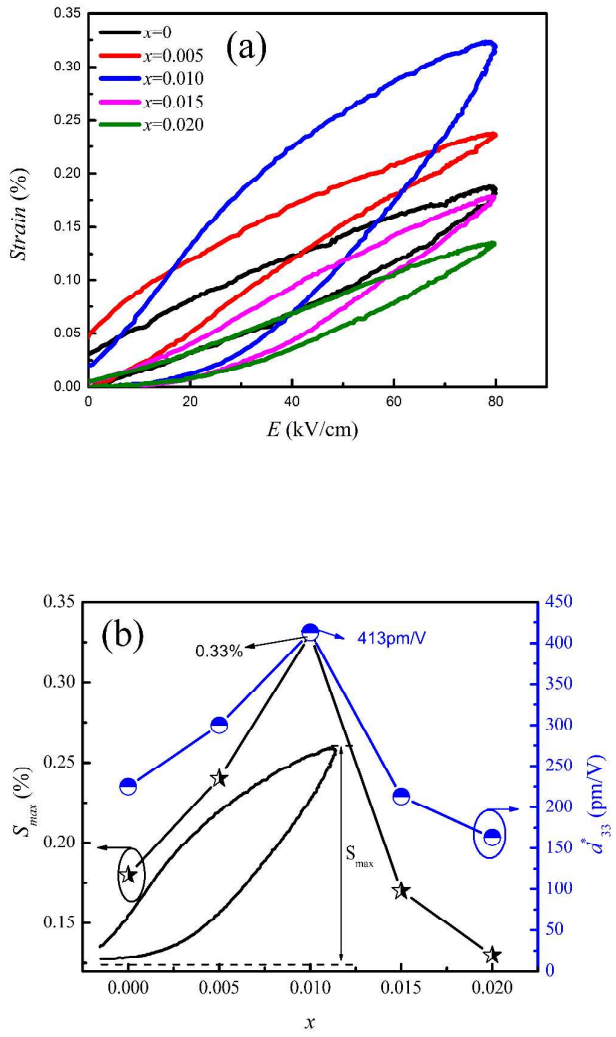

Fig. 7 (a) Unipolar field-induced strain curves of the BNT-BT6.5 ceramics with different AB contents, **(b)** Maximum strain and normalized strain ($d^*_{33} = S_{max} / E_{max}$) as a function of x in BNT-BT6.5-x AB ceramics

The unipolar electric field-induced strain curves for BNT-BT6.5-x AB ceramics with different x measured at room temperature are depicted in **Fig. 7 (a).** The unipolar field-induced strain level significantly increases with increasing x. The highest strain value (S_{max}=0.33%) is obtained for composition with x=0.010. However, a further increase in AB contents (x > 0.010) drops the strain level. The field-induced strain S_{max} and the normalized strain d^*_{33} of BNT-BT6.5-x AB ceramics as a function of x are presented in **Fig. 7(b)**. The enhanced strain (S_{max} = 0.33%), nearly two times more than that of

RSC Advances Accepted Manuscript

pure BNT-BT6.5 and the normalized strain ($d^*_{33} = S_{max}/E_{max}$ = 413 pm/V) were obtained for x = 0.010 at an applied electric field of 80 kV/cm. Recently, similar normalized strain behaviors were also observed in other BNT-based systems, such as BNT-BA,[33] BNT-BKT,[34] BNT-BT[35] and BNT-ST.[36, 37]

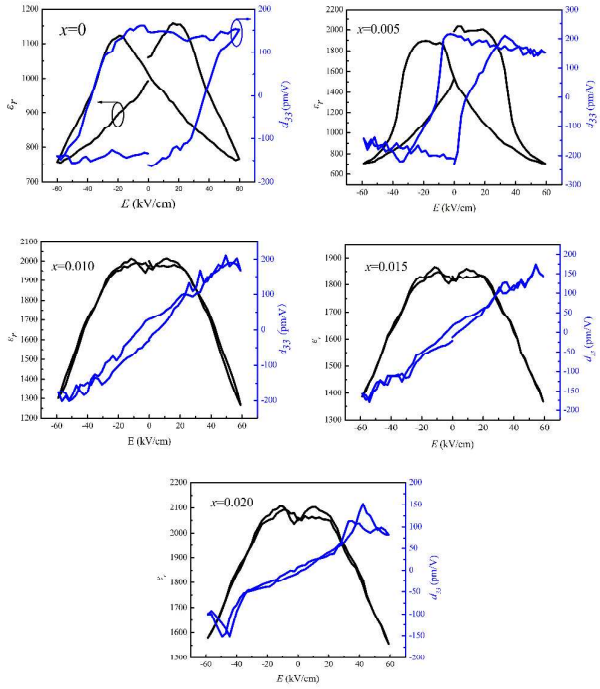

Fig. 8 Electric field dependences of ε_r and d_{33} for the BNT-BT6.5-x AB ceramics at 10 Hz

To further analyze the behavior under electric field, the d_{33}(E) and ε_r(E) of all samples were measured under an applied electric field of 60 kV/cm. As shown **Fig. 8**, the characteristics of both d_{33} (E) and ε_r(E) differ significantly for 0≤ x ≤0.005 and 0.010≤ x ≤0.020. As illustrated in **Fig. 8**, the relative dielectric constant ε_r(E) varies under the influence of an applied electric field. Compositions with 0≤ x ≤0.005 exhibit evident hysteretic behavior, which is closely connected to switching of ferroelectric domains. Before the coercive field is reached, the domain wall density increases, and hence permittivity increases as well. Due to the stress that is associated with the strain incompatibility of switching domains, clamping occurs, which results in a decrease of ε_r(E). In addition, the number of

RSC Advances Accepted Manuscript

domain walls diminishes at high field, and therefore hysteresis becomes smaller at higher fields. On the contrary, BNT-BT6.5-*x* AB samples (x≥0.010) display indiscernible hysteretic behavior, implying little domain switching[38]. Judging from the evolution of ε_r (E), it is evident that compositions with x≥0.010 keep permittivity high as in the undoped BNT-BT6.5 at zero electric field. In addition, it reduces the effect of the electric bias field on the permittivity, so that the relative deviation calculated through the maximum permittivity ε_{max}, the minimum permittivity ε_{min}, and the permittivity at zero field $\varepsilon_{0\mathrm{kV}}$ according to **Eq. (1)**[39] changes from 37% (x=0) to 78% (x=0.005), 36% (x=0.010), 26% (x=0.015) and eventually 25% (x=0.020). This result is in good agreement with *P*-*E* hysteresis loops.

$$\Delta\varepsilon=\frac{\varepsilon_{\max}-\varepsilon_{\min}}{\varepsilon_{0kV}} \quad (1)$$

The d_{33}(E) value of x=0 changes only slightly from its value of 134 pm/V at maximum field when the field is reduced to zero. In contrast, d_{33} for x=0.005 is 164 pm/V at 6 kV/mm and reaches a maximum at 33 kV/cm with 221 pm/V and then drops down to 212 pm/V at 0 kV/mm.

4. Conclusions

In summary, lead-free BNT-BT6.5-*x* AB piezoelectric ceramics were prepared by the conventional solid-state reaction method and the crystal structure, microstructure and electrical properties were systematically investigated. All BNT-BT6.5-*x* AB ceramics form the pure perovskite phase structure, SEM-analysis revealed an increase first and then decrease in the grain size with increasing AB content with no obvious change in grain morphology. With increasing AB content, the piezoelectric and ferroelectric properties of BNT-BT6.5-*x* AB ceramics first increase and then decrease. Improved P_r = 32.8 μC/cm^2, low E_c of 18.2 kV/cm, and high d_{33} = 234 pC/N were observed at x = 0.005. A large field-induced strain S_{max} =0.33%, corresponding to the normalized strain ($d^*_{33} = S_{max}/E_{max}$ = 413 pm/V), was obtained for x = 0.010. These results show that BNT-based ceramics modified with AB can be

RSC Advances Accepted Manuscript

considered superior candidate materials for lead-free practical applications.

Acknowledgments

This work was supported by the National Natural Science Foundation of China (No. 51372110, 51402144, 51302124), the National High Technology Research and Development Program of China (No. 2013AA030801), the Natural Science Foundation of Shandong Province of China (No. ZR2012EMM004), the Project of Shandong Province Higher Educational Science and Technology Program (No. J14LA11, No.J14LA10), Research Foundation of Liaocheng University (No. 318011301, No.318011306, No. 318051407)

References

1 T. Kudo, T. Yazaki, F. Naito and S. Sugaya, *J Am Ceram Soc*, 1970, **53**, 326-328.
2 H. Ouchi, K. Nagano and S. Hayakawa, *J Am Ceram Soc*, 1965, **48**, 630-635.
3 G. H. Haertling, *J Am Ceram Soc*, 1999, **82**, 797-818.
4 S.-E. Park and T. R. Shrout, *J Appl Phys*, 1997, **82**, 1804-1811.
5 Y. Li, K.-s. Moon and C. Wong, *Science*, 2005, **308**, 1419-1420.
6 P. Fu, Z. Xu, R. Chu, W. Li, W. Wang and Y. Liu, *Mater Des*, 2012, **35**, 276-280.
7 L. E. Cross, *Ferroelectrics*, 1994, **151**, 305-320.
8 T. Moriyama, A. Kan and H. Ogawa, *J Ceram Soc Jpn*, 2013, **121**, 644-648.
9 P. Du, L. Luo, W. Li, Y. Zhang and H. Chen, *J Alloy Compd*, 2013, **551**, 219-223.
10 D. Alonso‐Sanjosé, R. Jimenez, I. Bretos and M. L. Calzada, *J Am Ceram Soc*, 2009, **92**, 2218-2225.
11 Q. Wang, J. Chen, L. Fan, L. Liu, L. Fang and X. Xing, *J Am Ceram Soc*, 2013, **96**, 1171-1175.
12 J. Hao, C. Ye, B. Shen, J. Zhai, *J. Appl. Phys*, 2013,**114**, 054101.
13 P. Fu, Z. Xu, R. Chu, W. Li, G. Zang, J. Hao, *Mater Des,* 2010, **31**, 796–801.
14 J. Hao, B. Shen, J. Zhai, H. Chen, S. Zhang, *J Am Ceram Soc,* 2014, **97**, 1776–1784.
15 J. Hao, B. Shen, J. Zhai, H. Chen, *J Appl Phys*, 2014, **115**, 034101.
16 Z. Surowiak, J. Dudek, *J Mater Sci* 1991, **26**, 4407–4410.
17 T. Takenaka, H. Nagata, *J Eur Ceram Soc* 2005, **25**, 2693–2700.
18 W. Zhao, H.P. Zhou, Y.K. Yan, D. Liu, *Key Eng Mater,* 2008, **368,** 1908–1910.
19 H. Lidjici, M. Rguiti, F. Hobar, et al., *Ceram Silik*, 2010, **54**, 253–257.
20 P. Baettig, C. F. Schelle, R. LeSar, U. V. Waghmare and N. A. Spaldin, *Chem Mater*, 2005, **17**, 1376-1380.
21 A. A. Belik, T. Wuernisha, T. Kamiyama, K. Mori, M. Maie, T. Nagai, Y. Matsui and E. Takayama-Muromachi, *Chem Mater*, 2006, **18**, 133-139.
22 A. Ullah, C. W. Ahn, A. Hussain and I. W. Kim, *J Electroceram*, 2013, **30**, 82-86.
23 H. Yu and Z.-G. Ye, *Appl Phys Lett*, 2008, **93**, 112902.
24 Y. Zhen, S. Hall, T. Brown, E. Ekuma, Z. Bell, Z. Sun and J. Wang, *Ferroelectrics*, 2011, **413**, 192-205.
25 P. Fu, Z. Xu, R. Chu, X. Wu, W. Li and X. Li, *Mater Design*, 2013, **46**, 322-327.

RSC Advances Accepted Manuscript

26 S.-T. Zhang, A. B. Kounga, E. Aulbach, T. Granzow, W. Jo, H.-J. Kleebe and J. Rödel, *J Appl Phys*, 2008, **103**, 034107.

27 P. Fu, Z. Xu, R. Chu, W. Li, Q. Xie, Y. Zhang, Q. Chen, *J Alloy Compd*, 2010, **508**, 546-543.

28 H. Li, W. Yao, *Mater Lett*, 2004, **58**, 1194-1198.

29 M.K. Zhu, L.Y. Liu, Y.D. Hou, H. Wang, H. Yan, *J Am Ceram Soc,* 2007, **90**, 120–127.

30 L. X. He, G. Ming, C. E. Li, W. M. Zhu, H. X. Yan, *J Eur Ceram Soc*, 2001, **21,** 703–709.

31 W. Chen, Y.M. Li, Q. Xu, J. Zhou, *J Electroceram*, 2005, **15**, 229–235.

32 P. Fu, Z. Xu, H. Zhang, R. Chu, W. Li and M. Zhao, *Mater Design*, 2012, **40**, 373-377.

33 A. Ullah, C. W. Ahn, K. B. Jang, A. Hussain and I. W. Kim, *Ferroelectrics*, 2010, **404**, 167-172.

34 K. Yoshii, Y. Hiruma, H. Nagata and T. Takenaka, *Jpn J Appl Phys*, 2006, **45**, 4493.

35 S. T. Zhang, A. B. Kounga, E. Aulbach and Y. Deng, *J Am Ceram Soc*, 2008, **91**, 3950-3954.

36 W. Krauss, D. Schütz, F. A. Mautner, A. Feteira and K. Reichmann, *J Eur Ceram Soc*, 2010, **30**, 1827-1832.

37 Y. Hiruma, Y. Imai, Y. Watanabe, H. Nagata and T. Takenaka, *Appl Phys Lett*, 2008, **92**, 262904-262904-262903.

38 R. Dittmer, E. M. Anton, W. Jo, H. Simons, J. E. Daniels, M. Hoffman, J. Pokorny, I. M. Reaney and J. Rödel, *J Am Ceram Soc*, 2012, **95**, 3519-3524.

39 R. Dittmer, W. Jo, J. Daniels, S. Schaab and J. Rödel, *J Am Ceram Soc*, 2011, **94**, 4283-4290.

RSC Advances Accepted Manuscript